Enzyme and Microbial Technology 150 (2021) 109890

Contents lists available at ScienceDirect

Enzyme and Microbial Technology

journal homepage: www.elsevier.com/locate/enzmictec

# Structural studies of *Myceliophthora Thermophila* Laccase in the presence of deep eutectic solvents

Jou Chin Chan [a], Bixia Zhang [b], Michael Martinez [b], Balaganesh Kuruba [a], James Brozik [b], ChulHee Kang [b,**], Xiao Zhang [a,c,*]

[a] Voiland School of Chemical Engineering and Bioengineering – Washington State University, 2710 Crimson Way, Richland, WA, 99354, USA
[b] Department of Chemistry, Washington State University, Pullman, WA, 99164, USA
[c] Pacific Northwest National Laboratory - 902 Battelle Boulevard, P.O. Box 999, MSIN P8-60, Richland, WA, 99352, USA

ARTICLE INFO

*Keywords:*
Laccase
Deep eutectic solvent
Crystallization

ABSTRACT

In this work, we elucidated the interactions between *Myceliophthora thermophila* laccase and deep eutectic solvent (DES) by crystallographic and kinetics analyses. Four types of DESs with different hydrogen bond acceptor (HBA) and hydrogen bond donor (HBD), including lactic acid: betaine, glycerol: choline chloride, lactic acid: choline chloride and glycerol: betaine was used. The results revealed that different DES have different effects on laccase activity. Lactic acid-betaine (2:1) DES has shown to enhance laccase activity up to 300 % at a concentration ranged from 2% to 8% v/v, while glycerol: choline chloride and lactic acid: choline chloride DES choline chloride-based DES have found to possess inhibitory effects on laccase under the same concentration range. Detailed kinetic study showed that glycerol: choline chloride DES is a S-parabolic-I-parabolic mixed non-competitive inhibitor, where conformational changes can occur. The crystal structures of laccase with lactic acid: choline chloride DES (LCDES) were obtained at 1.6 Å. Crystallographic analysis suggested that the addition of LCDES causes changes in the laccase active site, but the increase in water molecules observed in the resulting crystal prevented laccase from experiencing drastic structural change. Fluorescence and circular dichroism spectroscopies were also applied to determine the effects of DES on the structural conformation of laccase. The results have confirmed that the presence of DES can trigger changes in the local environments of the amino acids in the active site of laccase which contributes to the changes in its activity and stability.

## 1. Introduction

The use of enzymes as biocatalysts has gained considerable interest, as it allows reactions to proceed in mild conditions, as well as having high selectivity and being nontoxic [1]. The improved knowledge base originates from intensive research work that has made large steps forward in the discovery of novel enzymes, advancement in protein engineering, and recombinant DNA technology. This has fueled ongoing research into making enzyme catalysis viable in industrial processes, along with the aim of moving towards green and sustainable chemistry.

One of the common industrial enzymes is laccase (EC 1.10.3.2, paradiphenol: dioxygen oxidoreductase). Laccase is a widely known member of the blue multicopper oxidase family, which can be found in fungi as well as in a variety of plants, bacteria, and insects [2–4]. In fungi, laccase participates in lignin degradation, pathogenesis, and detoxification, as well as development and morphogenesis [5,6]. Immense work has been carried out on laccase since its first discovery from the exudates of the Japanese lacquer tree *Rhus vernifera* (*Toxicodendron vernicifluum*) [7]. Laccase catalyzes the reduction of a variety of compounds including phenolic (mono-, di-, poly-, and methoxyphenols), nonphenolic, aromatic amines, aliphatic amines, benzenethiols, carbohydrates, and inorganic compounds, followed by the reduction of oxygen to water [8–12]. Although direct oxidation of phenolic compounds can take place, the oxidation of non-phenolic compounds by laccase requires the presence of a mediator due to steric hindrance or the high reduction potential of the substrate. Hence, a mediator that is usually made up of low molecular weight compounds acting as electron shuttler is necessary in the oxidation of non-phenolic compounds [13,14]. Interest in laccase has been stimulated by ongoing and potential applications in pulp and paper industries, environmental detoxification, food industries, textile

* Corresponding author at: Voiland School of Chemical Engineering and Bioengineering, Washington State University, Richland, USA.
** Corresponding author.
*E-mail addresses:* chkang@wsu.edu (C. Kang), x.zhang@wsu.edu (X. Zhang).

https://doi.org/10.1016/j.enzmictec.2021.109890

industries, and lignin valorization [15–21].

The first crystal structure of laccase was from *Coprinus cinereus* [22]. To date, there are more than 200 known laccase structures including complex structures with substrates, inhibitors, oxidation products, along with mutant structures deposited in the protein data bank (PDB). In general, laccases are primarily monomeric glycoproteins that contain four copper atoms in their active sites arranged into three metallocentres [23–26]. These metallocentres are located among three structural domains that are formed by a single polypeptide with approximately 500 amino acids in length [27]. The four copper centers are divided into Type 1 (T1), Type 2 (T2) and Type 3 (T3) copper according to their distinctive spectroscopic properties. T1 copper is responsible for the distinct blue colour with an absorption band at approximately 600 nm and T2 copper have an absorption shoulder at approximately 330 nm. In laccase, substrates are being oxidized at the mononuclear T1 copper site (reducing-substrate binding site) followed by the migration of electrons to the trinuclear cluster/copper site formed by the T2 and T3 coppers where the reduction of molecular oxygen to water took place [28,29].

The rapid emergence of alternative solvents has solved problems associated with the substrate solubility that hinders the application of biocatalytic reactions, such as applications of laccase. Consequently, deep eutectic solvents (DESs) have been brought into the limelight due to their appealing properties, including low volatility, a wide liquid range, nonflammability, high thermal stability, and tailored characteristics, as well as being biodegradable and low cost [30,31]. DESs are mixtures of salt and hydrogen bond donors in different molar ratios that produces a stable, homogeneous liquid phase at ambient conditions [32], which can be prepared by mixing the two precursors with continuous stirring for several hours at a moderate temperature without any purification requirements, thus forming minimal waste. Typical DESs are made up of readily available salts and are nontoxic and biodegradable, unlike other ionic liquids.

Studies indicate that DESs are less reactive in typical enzyme reaction systems due to the extensive hydrogen bond network that lowers the chemical potential of the individual components, which in turn makes DES applicable in a broad range of reactions [33]. In numerous studies, DES have been proven to stabilize and enhance the activity of enzymes [33–37]. Nevertheless, the understanding of the effects of DES on protein conformation and dynamics still remains unclear, although there are studies that demonstrate that DES can increase enzyme performance [37,38] and stability [39,40]. In this study, the detailed investigation of the three-dimensional crystal structure of laccase from the thermophilic fungus *Myceliophthora thermophila* is presented together with the discussion of the structure in the presence of DES. In addition, differential scanning calorimetry (DSC), fluorescence spectroscopy, and circular dichroism (CD) spectroscopy were carried out to provide insights on the enzyme conformation in the presence of DES.

## 2. Materials and methods

All chemicals used were of at least reagent grade and used without further purification unless otherwise specified. Sodium chloride (NaCl, CAS 7647−14-5), glacial acetic acid (CAS 64−19-7), Tris buffer (CAS 77−86-1), choline chloride (CAS 67−48-1), betaine (CAS 107−43-7), and glycerol (CAS 56−81-5) were purchased from Fisher Scientific while lactic acid (W261106) and 2′-azino-bis-3-ethylbenzathiazoline-6-sulfonic acid (ABTS) (A1888) were purchased from Sigma Aldrich. Protein molecular weight ladder (PageRuler™ Prestained Protein Ladder; 10 kDa–180 kDa, 26,616) was obtained from ThermoFisher. Screening solutions used for protein crystallization were obtained from Hampton Research.

### 2.1. Protein purification

membrane (Milipore) into buffer containing 100 mM sodium acetate pH 5 and further purified with an AKTA FPLC system (GE Healthcare). 200 μL of the buffer-exchanged and concentrated sample was then loaded to a Superdex 200 Increase 10/300 G l column (GE Healthcare, 28−9909-44, column L × I.D. 30 cm ×10 mm, 8.6 μm particle size) that had been pre-equilibrated with 50 mM sodium acetate pH 5 buffer containing 0.15 M sodium chloride (NaCl). Proteins were eluted in 0.5 mL fractions with the equilibration buffer at a flow rate of 0.5 mL/min. Sodium dodecyl sulfate polyacrylamide gel electrophoresis (SDS-PAGE) was used to check the purity of the collected fractions. Then, the purified fractions were pooled, re-concentrated (Amicon 8050 ultrafiltration cell, 30 kDa cutoff membrane) and stored at 4 °C for further characterization and analysis. Bradford procedure was used to measure the protein concentration, using bovine serum albumin as the standard with 50 mM Tri−HCl pH 5 with 0.15 M NaCl buffer as the diluent [41].

### 2.2. Protein purity

The molecular mass of the purified laccase was determined by performing sodium dodecyl sulfate polyacrylamide gel electrophoresis (SDS-PAGE). SDS-PAGE was performed with 12 % polyacrylamide gel by the Laemmli method [42] with Precision PlusProtein™ Kaleidoscope™ standard (BioRad) as the molecular weight marker. The gel was stained with staining solution that contains 0.1 % (v/v) Coomassie Brilliant Blue R-250, 40 % (v/v) methanol and 7% (v/v) glacial acetic acid for 2 h with mild agitation and de-stained with de-staining solution that contains 10 % methanol with 10 % acetic acid solution overnight or until a clear background was achieved.

### 2.3. Molecular mass determination

0.73 mg $ml^{-1}$ (9.2 u M) in 100 μL of the re-concentrated sample was loaded on to a Yarra 3 um SEC 2000 column (Phenomenex) and eluted with 20 mM MOPS buffer pH 7.0 with 0.15 M sodium chloride, 0.05 g/dl sodium azide ($NaN_2$). The eluate was passed in tandem through the UV detector (Gilson), refractometer (Optilab DSP, Wyatt Technology), and the multi-angle laser light scattering detector (Dawn EOS, Wyatt Technology). The light scattering data was analyzed with Astra software (Wyatt Technology Corp.) using the Zimm fitting method.

### 2.4. Preparation of deep eutectic solvents

The deep eutectic solvents (hereby defined as DESs) used in this study were prepared from lactic acid and choline chloride (LCDES, molar ratio 2:1), lactic acid and betaine (LBDES, molar ratio 2:1), glycerol and choline chloride (GCDES, molar ratio 2:1), and glycerol and betaine (GBDES, molar ratio 2:1). The mixtures were heated at a 60 °C and stirred with a constant stirring rate of 200 rpm until a homogenous solution was obtained. The density of DESs were measured gravimetrically in triplicate and the average values were recorded to ensure the accuracy and reproducibility of the collected data.

### 2.5. Laccase activity assay

The enzyme activity was determined spectrophotometrically using a UV–vis spectrophotometer (Genesys™ 10S UV–vis, Thermo Scientific, USA) with 2,2′-azino-bis-3-ethylbenzathiazoline-6-sulfonic acid (ABTS) as the substrate. The assay was carried out at room temperature (25 °C) with 100 mM sodium acetate pH 5 with 0.15 M NaCl. The reaction mixture (1 mL) consists of 0.02 mg $ml^{-1}$ purified laccase, 0.5 mM ABTS with or without DES (0–8 % v/v). The enzyme activity was computed form the increase in A420. The molar extinction coefficient of ABTS is 36,000 $M^{-1}$ $cm^{-1}$. One unit of enzyme activity is defined as the amount

mean ± standard deviation of the results was calculated to ensure the repeatability and reproducibility of the obtained results.

### 2.6. Kinetic studies of laccase with GCDES

The kinetic studies were conducted with 25–150 μM for GCDES. Similarly, the concentration of the reaction mixture was 100 mM sodium acetate at pH 5, 0.005 mg of enzyme, and different concentrations of GCDES (% volume) in a total reaction volume of 250 μL. ABTS was freshly prepared before each experiment. The mixture was incubated for 5 min at room temperature prior the addition of substrate to start the reaction. The absorbance was measured immediately in 20 s intervals for 15 min.

Kinetic data were fit into the appropriate rate equations using OriginPro. The enzyme kinetic parameters, $V_{max}$ and $K_m$, were determined by nonlinear hyperbolic curve fitting to the Michaelis-Menten equation. Likewise, all kinetic assays were performed in at least triplicate to ensure the repeatability and reproducibility of the obtained results. Dixon plots were frequently used to identify the types of inhibition as well as determining the $K_i$ value. When both the $V_{max}$ and $K_m$ are affected by the reaction with the presence of inhibitor, the inhibitor is referred as a mixed-type inhibitor. Eq. 1 was used to plot the Dixon plot where $K_i$ is the inhibitor's binding constant for the noncompetitive site and α is the factor that describes the difference in affinity of the inhibitor at the same site of the enzyme-substrate complex. The slope of the Dixon plot is shown is Eq. 2. The plot of slope versus 1/[S] was plotted in order to determine the values of $K_i$ and α if the Dixon plot displayed a linear behavior. However, if the Dixon plot yields a parabolic pattern, the initial rate data were then plotted as 1/V versus 1/S. A parabolic behavior of the Dixon plot will yield a Lineweaver-Burk plot that consist of straight lines without a common intersecting point. Eq. 2 and Eq. 4 are the reciprocal equation that describe classical competitive inhibition, classical non-competitive inhibition.

$$\frac{1}{v} = \frac{\left(1 + \frac{\alpha \cdot K_m}{[S]}\right)}{\alpha \cdot K_i \cdot V_{max}} \cdot [I] + \frac{1}{V_{max}}\left(1 + \frac{K_m}{[S]}\right) \quad (1)$$

$$slope = \frac{K_m}{K_i \cdot V_{max}} \cdot \left(\frac{1}{[S]}\right) + \left(\frac{1}{\alpha K_i V_{max}}\right) \quad (2)$$

$$\frac{1}{v_0} = \frac{K_m}{V_{max}}\left(1 + \frac{[I]}{K_i}\right)\frac{1}{[S]} \cdot + \frac{1}{V_{max}} \quad (3)$$

$$\frac{1}{v_0} = \frac{K_m}{V_{max}}\left(1 + \frac{[I]}{K_i}\right)\frac{1}{[S]} \cdot + \frac{1}{V_{max}}\left(1 + \frac{[I]}{K_i}\right) \quad (4)$$

The data were plotted using the replot of slopes and intercept versus 1/[S] to determine if a non-linear inhibition present. The secondary plot will have a linear pattern if system is a pure noncompetitive inhibition with a single inhibition site. However, if a parabolic pattern was observed from the secondary plot, this indicates a complex non-competitive inhibition system with multiple inhibition sites or structural conformational changes [43]. There are several forms of parabolic inhibition. It can be parabolic competitive, S-linear I-parabolic noncompetitive, S-parabolic I-linear noncompetitive and S-parabolic I-parabolic noncompetitive inhibition. The reciprocal form of these types of inhibition are shown in Eq. 5 to Eq. 8, respectively. Eq. 9 is modified form of Eq. 8 for S-parabolic I-parabolic noncompetitive inhibition [44,45].

$$\frac{1}{v_0} = \frac{K_m}{V_{max}}\left(1 + a[I] + b[I^2]\right)\frac{1}{[S]} \cdot + \frac{1}{V_{max}} \quad (5)$$

$$\frac{1}{v_0} = \frac{K_m}{V_{max}}\left(1 + a[I] + b[I^2]\right)\frac{1}{[S]} \cdot + \frac{1}{V_{max}}(1 + c[I]) \quad (7)$$

$$\frac{1}{v_0} = \frac{K_m}{V_{max}}\left(a + b[I] + c[I^2]\right)\frac{1}{[S]} \cdot + \frac{1}{V_{max}}\left(d + e[I] + f[I^2]\right) \quad (8)$$

$$\frac{1}{v_0} = \frac{K_m^*}{V_{max}}\left(1 + g[I] + h[I^2]\right)\frac{1}{[S]} \cdot + \frac{1}{V_{max}}\left(1 + j[I] + k[I^2]\right) \quad (9)$$

where $K_m^*$ is the limiting $K_{max}$for S at the fixed concentration of all the nonvaried ligands in the absence of [I]. Eq. 10 and Eq. 11 were applied to plot the slope and intercept of S-parabolic I-parabolic inhibition [44].

$$slope = \frac{K_m^*}{V_{max}^*}\left(1 + g[I] + h[I]^2\right) \quad (10)$$

$$\text{int} = \frac{K_m^*}{V_{max}^*}\left(1 + j[I] + k[I]^2\right) \quad (11)$$

When apparent parabolic lines are obtained, the parabolic nature of the curves was confirmed by the replot of the data against the square of the reciprocal of substrate concentration or the concentration of the inhibitor.

### 2.7. Differential scanning calorimetry (DSC)

The structural stability and melting point of *M. thermophilla* laccase with different DESs were determined by differential scanning calorimetry (DSC) using a DSC scanning calorimeter (NETZSCH DSC 214 Polyma). Approximately 20 mg of *M. thermophila* laccase samples (20 μL) in 50 mM sodium acetate buffer pH 5 was sealed in a Netzsch Concavus aluminum pan with pierced lids (tiny hole punched in the upper lids) that was previously weighted (control sample). For the effects of DES on the thermostability of the *M. thermophila* laccase, 5 % v/v of LCDES, LBDES, GCDES and GBDES were incubated with the protein for at least 20 min prior to the DSC analysis. The reference pan in each case was an empty sealed Concavus aluminum pan with pierced lids. Pure nitrogen was used as the purge gas at a flow rate of 40 ml $min^{-1}$. The scanning begins at 20 °C and heated to 95 °C at a heating rate of 1 °C $min^{-1}$. Cooling was achieved with liquid nitrogen with a cooling rate of 10 K $min^{-1}$. Baseline corrections were carried out by subtracting the buffer thermogram. The maximum melting point ($T_m$, peak temperature) was recorded based on the achieved DSC curve. Data obtained were analyzed using Netzsch Proteus Thermal Analysis software.

### 2.8. Crystallization of Myceliophthora thermophila laccase

Initial crystallization studies were carried out at 295 K by screening with crystal screening kits from Hampton Research (Crystal Screen 1, Crystal Screen 2) using Phoenix /RE crystallization robot (Art Robbins Instrument, USA) with a protein concentration of 30 mg $ml^{-1}$. Prior to crystallization, the purified protein was buffer exchanged to 20 mM sodium acetate buffer pH 8 and concentrated to a concentration of 100 mg $ml^{-1}$. All crystallization trials were conducted in a hanging drop vapor diffusion setup at 295 K. Blue crystals appeared within a week in condition containing 0.1 M HEPES pH 7.45, 0.22 M calcium chloride, 0.05 M glycine and 34 % polyethylene glycol 400. Fully grown crystals are soaked in cryoprotectant that contains 20 % (v/v) glycerol in the reservoir solution and mounted on a nylon loop before shipping to the Berkeley Advanced Light Source (ALS) in liquid nitrogen. Data sets were processed and scaled using HLK-2000 [46].

### 2.9. Data collection

the ALS and processed (indexed, integrated and scaled) using software package HLK-2000 [46]. PHENIX Phaser was used to performed molecular replacement for the initial phasing with the structural coordinates of laccase from *Myceliophthora thermophila* (PDBI: 6F5K). Refinement and model building were done using PHENIX and Coot [47]. Detailed description of the crystallization and data collection process can be found in Section A in the Supplementary information.

### 2.10. Fluorescence spectroscopic analysis

Intrinsic fluorescence spectra were recorded with a spectrofluorometer (Photon Technology International, PTI QuantaMaster 8000). Purified *M. thermophila* laccase at 0.1 mg $ml^{-1}$ concentration in 50 mM sodium acetate buffer containing 0.15 M NaCl were excited at 295 nm for intrinsic tryptophan fluorescence. The fluorescence emission spectra were recorded with a 1.0 cm quartz cell over the wavelength range of 300 nm–400 nm at a scanning interval of 1 nm, slit width fixed 1 nm and integration time of 1 s (averaging three scans) using 50 mM sodium acetate buffer containing 0.15 M NaCl as a control. All spectra were obtained using OriginPro through baseline corrected with the respective buffers by subtraction.

### 2.11. Circular dichroism spectroscopy

The CD spectra of the laccase solution in the presence of DESs were measured using an Aviv model 400 spectropolarimeter (Lakewood, NJ). *M. thermophila* laccase (0.12 mg $m^{-1}$l) in 50 mM sodium acetate buffer pH 5 were recorded at 25 °C under a $N_2$ atmosphere. The spectrum was recorded between 250 nm to 200 nm using a 1 mm cuvette. Spectra measurements below 200 nm were not feasible because the dynode voltage reached values greater than 500 mV. Data points were collected with a 0.5 nm interval with a 1 nm bandwidth and with an averaging time of 5 s. The spectra obtained for each sample were corrected by subtraction of the signal obtained for the buffer containing respective concentration of GCDES.

## 3. Result and discussion

### 3.1. Laccase activity in different DESs

The list of DESs used in this study with their respective abbreviations and properties is shown in Table 1. The enzyme activity of purified *M. thermophila* laccase (Fig. S1) in the presence of varying concentrations of different DESs using ABTS as the substrate in 50 mM sodium acetate buffer pH 5 is shown in Fig. 1. Lactic acid-containing DES has produced the most pronounced effect on the enzyme activity, where the activity is drastically enhanced to a maximum of 300 % when 8 % v/v of LBDES is used. Similarly, the enzyme also performed well in the presence of LCDES, where an increase of at least 120 % was observed. The addition of different concentration of GBDES has shown a consistent increase in laccase activity (approximately 130 %) while a slight decrease in activity was observed in different concentration of GCDES. However, the decrease in laccase activity is mild where the laccase activity is maintained above 80 % for all GCDES concentrations.

It has been reported that the presence of solvents, particularly solvents that are homogenous phases with the buffer solution, substantially

**Table 1**
List of DES used in this study.

| DES | Density (g $cm^{-3}$) | HBD | Salt | Molar ratio | |
|---|---|---|---|---|---|
| | | | | HBD | Salt |

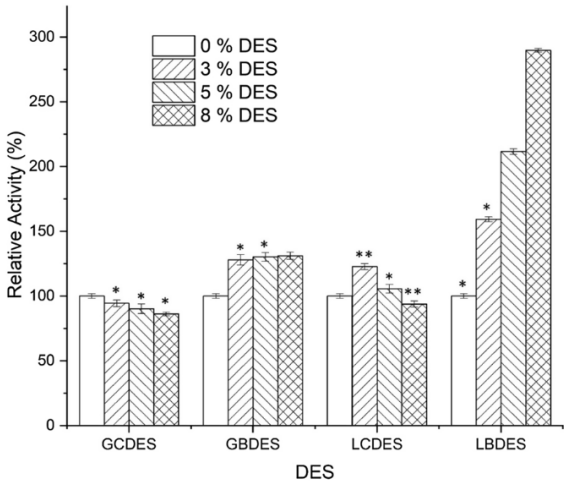


**Fig. 1.** Relative activity of *M. thermophila* laccase in the presence of different compounds, the activity of *M. thermophila* laccase without additives was defined as 100 %. The significant difference (*) was set at $P < 0.05$ and the highly significant difference (**) was set at $P < 0.01$ in Student's t-test, compared to the control. Data were shown as mean ± standard errors of the mean from at least three independent repeats.

affect the activity, stability, and structure of the biocatalyst through the interaction of the solvent with the protein molecules or the modification of the thermodynamic water activity [48,49]. Several studies indicate that the enzymatic performance in DES varies according to the types of hydrogen-bond acceptor (HBA) and hydrogen-bond donor (HBD) as well as their molar ratio where it substantially affects the solvent properties including the polarity, viscosity, and surface tension, which in turn influences the enzyme's activity and the overall stability of the reaction [33,36,50]. The changes in solvent properties when DES is incorporated into the reaction are due to the existence of a hydrogen bond network in DES, which can increase the rate of enzyme affinity to the substrate and influence on conformational stability of enzymes. In general, the helical conformation in the enzymes is protected by the hydrogen bonds in DES, preventing ions from penetrating into the individual domains of the enzyme. For instance, molecular dynamics simulation showed that the α-helix in lipase was preserved when it was exposed to reline (commercial name of the mixture of choline chloride-urea deep eutectic solvents) where the choline chloride and urea molecules formed superstructures through hydrogen bonds, which obstructed the diffusion of the urea molecules. In the absence of choline chloride, denaturation of the α-helix occurs as urea molecules readily diffuse into the protein core and disrupt the intramolecular hydrogen bonds, forming new hydrogen bonds with the residues constituting the helix [51]. Being the intrinsic characteristics of DES, the hydrogen bond network allows the DES molecules to interact with enzyme by docking the enzyme molecule into the DES network, subsequently stabilizing the protein.

It is notable that there is a remarkable increase in the laccase activity in the presence of LBDES. Studies have revealed that the HBDs that have a higher tendency to form hydrogen bonds, tends to improve enzyme activity compared to HBDs that have a lower tendency to form hydrogen bonds. Hence, it can be deduced that LBDES has the strongest ability to form hydrogen bonds, leading to the highest increase in enzyme activity. The detailed study about the characteristics of hydrogen bond between lactic acid and betaine DES revealed that the hydroxyl group of lactic acid interacts with the carboxylate group in betaine, in addition to the interactions between the methyl groups present in betaine with the oxygen atoms present in lactic acid [52]. Radial distribution functions

carbonyl group [52]. Self-hydrogen bonding was also present between lactic acids (LA—LA) as well as betaine-betaine interactions through methyl and carboxylate groups. Hence, the enormous increase in *M. thermophila* laccase activity in the presence of LBDES in this study can be attributed to the multiple hydrogen bonds in LBDES through various interactions.

Similarly, from the increase of laccase activity observed in the presence of GBDES, it is clear that the number of hydrogen bonds present in GBDES contains the betaine-betaine hydrogen bonds in addition to the glycerol-betaine hydrogen bonds. Previous studies also demonstrated that betaine-based DES has the ability to enhance both the stability and activity of the enzyme besides preventing protein denaturation [34,53–56]; while glycerol also often acts as a protein stabilizer that increases the α-helix content and reduces the β-sheet of the protein, improving the enzyme activity [57–59]. The minor decrease in enzyme activity in the presence of GCDES is due to the presence of chloride anions originating from choline chloride, which is a known inhibitor of laccase. However, the inhibitory effects of chloride ions are substantially diminished due to the formation of hydrogen bonds with glycerol. Based on the aforementioned RDF studies [52], it is reasonable to infer that self-hydrogen bond exists between lactic acid aside from the hydrogen bonds formed among lactic acid and choline chloride in LCDES. These additional hydrogen bonds could contribute significantly to the evident elevation of enzyme activity. Likewise, it is reasonable to deduce that the activation effects of LCDES are being suppressed by the presence of chloride anion in increasing concentration of LCDES. Finally, it may be concluded that the amount of hydrogen bonds present in these DESs establish the following the order; LBDES > LCDES > GBDES > GCDES, which results in different stimulation/inhibition effects on the enzyme activity.

### 3.2. Kinetic analysis

In this study, the inhibitory effects of GCDES on *M. thermophila* laccase were investigated. A regular spectrophotometric assay was performed (without DES) as a control and the assay was continued with different concentration of ABTS. Similarly, *M. thermophila* laccase was first incubated with the inhibitor (GCDES solution) for at least 5 min for all concentrations (1 %–5 % v/v). Assays were carried out where the reaction rates of the *M. thermophila* laccase with ABTS (25 μM – 100 μM) were measured over a range of GCDES concentrations (1 % v/v - 5 % v/v); the results were plotted as weighted double reciprocal plots (inversed rate obtained from different substrate concentrations plotted against inversed substrate concentration) with slopes and intercept replots. The shape of these plots will provide specific information on the mechanism of inhibitions.

The double reciprocal Lineweaver-Burk plot (1/V vs 1/S) generated straight lines at varying concentrations of GCDES where part of the lines intersected in the second quadrant without a common intersecting point (nonintersecting linear noncompetitive), as illustrated in Fig. 2. Both the slope and intercept change conspicuously at increasing concentration of GCDES (0–5%, 0–108 μM), indicating GCDES induced a mixed inhibition mechanism in *M. thermophila* laccase. The varying slopes and abscissa intercepts in the plots indicated that GCDES is a noncompetitive inhibitor with respect to ABTS, where GCDES does not compete with ABTS for the active site but affects the other binding sites that interfere with the binding of ABTS. The potential hydrogen bond interaction in the GCDES (between glycerol and choline chloride) may possibly lower the affinity between ABTS and laccase active site, causing an increase in apparent $K_m$ when the concentration of GCDES increases. The values of apparent $K_m$ and $V_{max}$ for different concentrations of GCDES are listed in Table 2. The apparent $V_{max}$ ($V_{max}^{app}$) decreased with the increase in GCDES concentration, while the apparent $K_m$ ($K_m^{app}$) fluctuates and

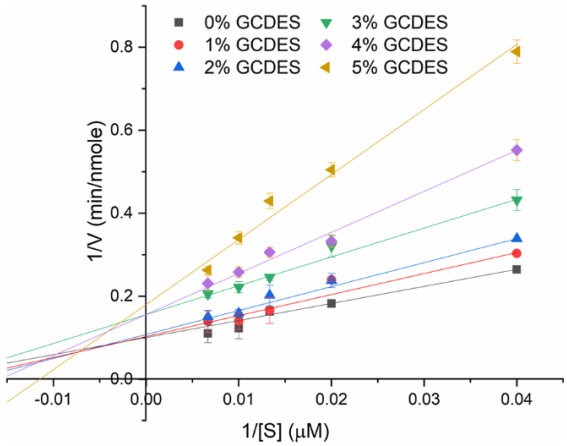


**Fig. 2.** Lineweaver-Burk plot for kinetic analysis of *M. thermophila* laccase inhibition by GCDES.

**Table 2**
Apparent $K_m$ and $V_{max}$ values for different concentrations of GCDES.

| % GCDES (v/v) | $V_{max}^{app}$ (nmoles $min^{-1}$) | $K_m^{app}$ (μM) |
|---|---|---|
| 0 | 11.493 ± 0.5 | 52.151 ± 2.0 |
| 1 | 10.559 ± 0.3 | 55.843 ± 2.8 |
| 2 | 9.060 ± 0.2 | 50.973 ± 2.3 |
| 3 | 6.953 ± 0.1 | 50.003 ± 2.6 |
| 4 | 6.082 ± 0.5 | 58.016 ± 3.5 |
| 5 | 5.202 ± 0.3 | 79.011 ± 2.2 |

($intercept_{LB}$ versus [GCDES]) (Figs. 3 and 4 ) were constructed from the data of the double reciprocal Lineweaver-Burk plot in Fig. 2. It showed a parabolic pattern where the graph curved upwards with concavity. The parabolic behavior of the replots indicates that the inhibition is a nonlinear parabolic non-competitive type (S-parabolic I-parabolic noncompetitive) of inhibition where S represents the slope and I represents the intercept [44,45]. This further confirms that GCDES follows a partial inhibition mechanism as pure noncompetitive inhibition would yield linear replots. The nonlinear noncompetitive pattern suggests that there is more than one molecule of GCDES binding on the enzyme and contributing to the inhibition mechanisms where the enzymatic complexes result in a complex interaction with laccase. Employing the curve fitting method, both the slope and intercept plots can be described by a

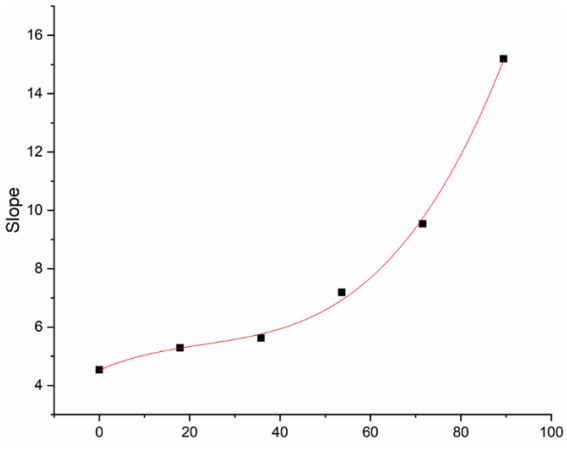

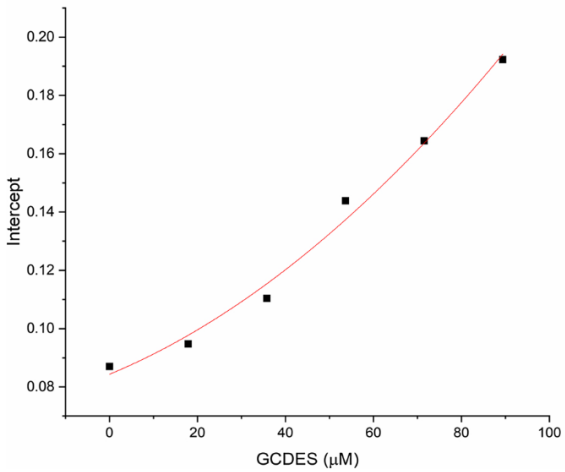


**Fig. 4.** Replot of intercepts of the Lineweaver-Burk plots against the concentration of GCDES.

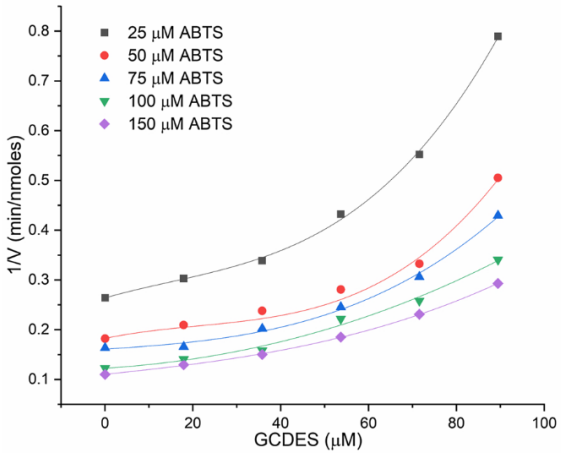


**Fig. 5.** Dixon plot of *M. thermophila* laccase at fixed ABTS concentration with varying concentration of GCDES.

second order polynomial equation with respect to GCDES, where a parabolic equation with a correlation coefficient of 0.98 and 0.99 respectively for slope replot and intercept replot was obtained. Third order polynomial fitting resulted in 0.99 correlation coefficient, but this is not considered in this study due to the complexity of the model. Hence, based on the fit, the two molecules of GCDES binds to the free enzymes (forming $EI^2$) and enzyme-substrate complex ($ESI^2$). The proposed reaction mechanism and the respective equation reaction is shown in Table 3. From the proposed mechanism, both models allowed the binding of two inhibitor molecules to the ESI complex which are the possible scenarios of the reaction of laccase with ABTS as the substrate and GCDES as the inhibitor.

The presence of two mutually exclusive binding sites (multisite inhibition system) at the enzyme was shown in the parabolic pattern of Dixon plot (1/V versus [I] at a fixed concentration of ABTS) (Fig. 5). The curve became increasingly parabolic with decreasing ABTS concentrations. The parabolic behavior of the Dixon plot makes is unsuitable for the determination of the binding constant of the inhibitor ($K_i$). In this type of inhibition, the inhibitor interacts with the enzyme at the active site as well as other binding sites [44]. Evidently, GCDES acts as a nonlinear noncompetitive mixed inhibitor where it interacts with the residue surrounding the enzyme active site, thus preventing the binding of substrate; the inhibitor also interacts with the enzyme at a different binding site and induce structural changes in the enzyme, resulting the enzyme-substrate complex inactive in the reaction system of *M. thermophila* laccase. Two non-mutually exclusive inhibitor binding sites exists in laccase and the binding of inhibitors will eventually lead to the formation of abortive complexes where no product can be formed. Consequently, parabolic inhibition is always a complete inhibition, as saturating concentrations of inhibitor will ultimately drive all enzymes into abortive complexes. The S-parabolic I-parabolic inhibition was modelled using Matlab™ according to the equation provided by Leskovac (2003) to obtain the constant of the velocity equation (Eq. 8, supplementary information) [45]. The full equation with values obtained from the software is as shown in Table S1 with an $R^2$ value of 0.95. The constants *a–f* are interaction factors that represent the effects of inhibitor binding on EI, ESI, IEI, and multiple inhibitors (I) on E

**Table 3**
Mixed noncompetitive inhibition models where E = enzymes, S = substrate, I = inhibitor. Modified from [60].

| | Proposed mechanism |
|---|---|
| 1 | 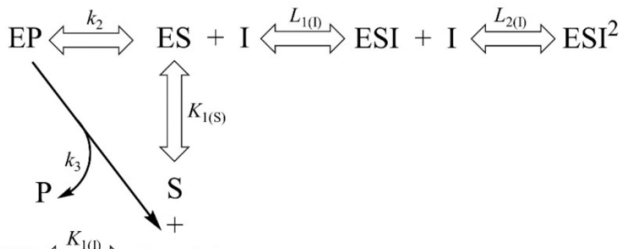 |
| 2 | 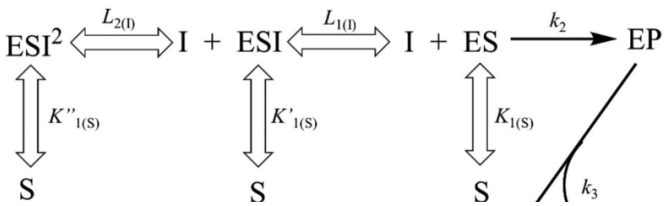 |

complexes upon GCDES exposure.

### 3.3. Differential scanning calorimetry

The thermal stability of *M. thermophila* laccase was studied in 5 % v/v of LCDES, LBDES, GCDES and GBDES, respectively. In general, the extent of hydrogen bonds, free volume, and the hydration level of the structure in DES can affect the thermostability of the protein. The increase in thermal stability of the protein is reflected by an increase in the thermal transition temperature $T_m$ (the maximum of each thermogram curve where $T_m$ corresponds to the temperature that causes the protein to unfold) and the transition of a protein from its native state to the denatured state is accompanied by the rupture of both the intramolecular bonds and intermolecular bonds. Table 4 showed that *M. thermophila* laccase denatured at 86.7 °C in 50 mM sodium acetate buffer pH 5. The thermal stability of *M. thermophila* laccase increases the most in the presence of LBDES, where the $T_m$ is 88.5 °C, followed by LCDES with a $T_m$ of 88.0 °C, GCDES with a $T_m$ of 87.4 °C, and GBDES with a $T_m$ of 86.9 °C. The best degree of protein stabilization was achieved in the presence of LBDES. Generally, all four DES have a stabilizing effect on *M. thermophila* laccase.

### 3.4. Structural studies of M. thermophila laccase with LCDES

Attempts to crystallize DES with laccase were carried out by soaking the crystal with DES before flash freezing to investigate the effects of DES on the protein structure. The crystal structure of the APO protein was obtained at 1.5 Å (Fig. S2) and its refinement statistics is shown in Table S2. The calculated molecular weight without the carbohydrates is 67.6 kDa and the molecular weight obtained from analytical size exclusion chromatography (multiangle light scattering, MALS) is 115 kDa for the single chromatographic peak observed by analytical size-exclusion chromatography (Fig. S3). Fig. 6 illustrates the protein structure of the protein crystal soaked with LCDES (1.7 Å) after structural alignment with apo-protein (1.5 Å) and removing the overlapped molecules. From Fig. 6, it is noticed that there is an increase in the number of bound water molecules in the structure, located in both the surface as well as the interior of the enzyme, forming a hydration layer around the protein. The increase in the number of water molecules can be seen in Table 5, which also showed the change in the unit cell dimension upon exposing to DES.

The changes in root mean square deviation (RMSD) of the crystal with DES are shown in Table 6. It is notable that the changes in domain-I and domain-III are more apparent, compared to the changes of RMSD in domain-II. The backbone of the protein is minimally changed, indicating that the backbone of the protein is unable to interact with the organized water molecules around the DES, similar to the reported results [61]. From the apo-structure of laccase, the mononuclear copper center (T1 copper) of *M. thermophila* laccase is located in domain-III, being the primary electron acceptor site where laccase catalyzes four one electron oxidations of a reducing substrate. The trinuclear cluster (T2 and T3) is positioned at the interface between domain-I and domain-III, where domain-III contributes to the formation of the trinuclear copper center binding site. Studies showed that domain-III in multicopper oxidase comprises of the putative substrate-binding site that is located on the surface of the protein close to the mononuclear copper center [62],

**Table 4**
Melting temperature of *M. thermophila* laccase in different DESs.

| Types of DES | Melting temperature, $T_m$ (°C) |
|---|---|
| Control | 86.7 ± 0.06 |

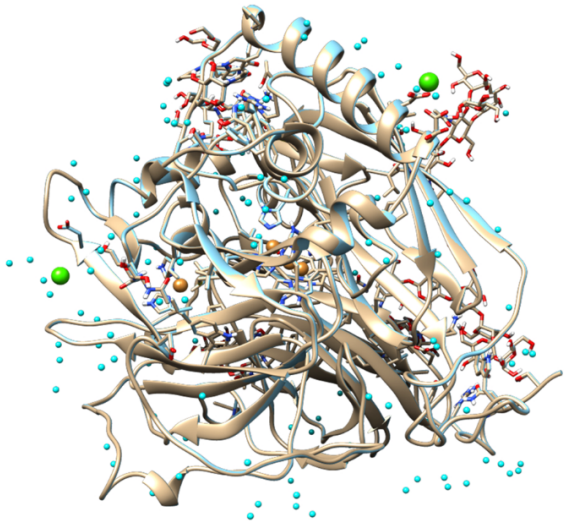

**Fig. 6.** Crystal structure of *M. thermophila* laccase (APO, brown) and with LCDES (cyan) after matching after removing the overlapped water molecules. Copper ions are shown as brown spheres and calcium ions (present in the crystallization solution) are shown as green spheres (For interpretation of the references to colour in this figure legend, the reader is referred to the web version of this article).

**Table 5**
Changes of crystal with addition of DES.

| Description | Unit cell: a, b,c | Resolution (Å) | No. of water molecules | RMSD |
|---|---|---|---|---|
| APO | 67 129 163 | 1.49 | 449 | – |
| 15 % v/v LCDES | 67 128 163 | 1.64 | 532 | 0.062 |
| 25 % v/v LCDES | 67 130 165 | 1.78 | 481 | 0.1 |

**Table 6**
Changes in root mean square deviation.

| Description | Whole | Backbone | Domain | | |
|---|---|---|---|---|---|
| | | | I | II | III |
| 15 % v/v LCDES | 0.350 | 0.062 | 0.065 | 0.049 | 0.059 |
| 25 % v/v LCDES | 0.432 | 0.1 | 0.106 | 0.075 | 0.102 |

which is consistent with the aforementioned potential binding sites of ABTS. The RMSD obtained shows more changes occurred in the trinuclear active site of the protein in the presence of DES (Fig. 7). The crystallographic data collection and refinement statistics for *M. thermophila* laccase with LCDES is shown in Table S3.

Crystals of protein generally contain up to 70 % of water, which reflects a wide range of nonrandom hydrogen bonding environment [63]. In typical lattice of protein crystals, some of the waters are in fixed positions and are observed every time the structure is determined, while others are in nonunique positions, reflecting the water-protein interactions that hydrates either the surface or the protein core. Generally, the stability, structure and function of the protein are influenced by the surrounding water molecules, through solvation and hydrophobic effects as well as the formation of specific hydrogen bonds [63–65]. In other words, protein dynamics and activity were affected by solvent dynamics. The additional water molecules observed in the presence of

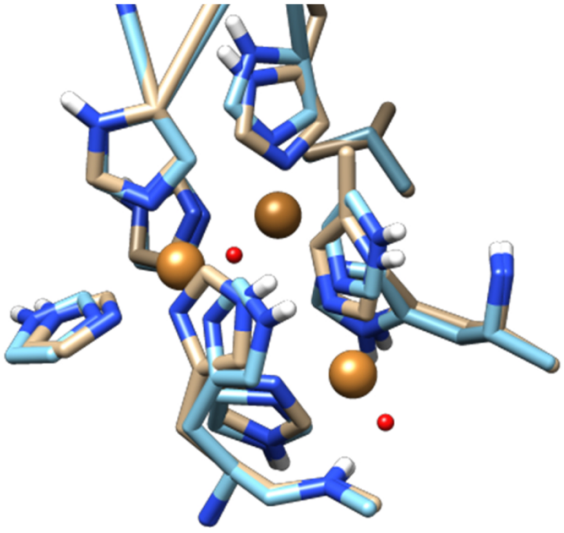

**Fig. 7.** Changes in the amino acids surrounding the trinuclear copper cluster in the presence of LCDES (cyan colored structure).

the structural and thermal stability of the protein [61,66]. The obtained crystal structure substantiated the previous speculations stating a hydration layer was formed around the protein when DES is added. This structural data is well-correlated to the activity and stability data justifying that DES is able to facilitate the enzyme stability and activity.

In addition, water molecules also act as a lubricant that ease the changes of hydrogen bonding patterns responsible for drastic conformational changes [67,68], which is in agreement with the obtained result which showed that there is a significant alteration in the unit cell of the crystal lattice of laccase but without drastic structural changes in the presence of DES. The strong hydration of the protein residues promotes the existence of a peptide/solvent interface where the intermolecular hydrogen bonds insert the surface structure of the protein into the water-hydrogen bond network, leading to increase catalytic activity and enhanced stabilization of the protein [69–71]. It is important to note that that it is the amount of water associated with the enzyme rather that the total water content in the reaction system that affects the catalytic activity of the enzyme, which can be quantify by the thermodynamic water activity ($a_w$) parameter. It is therefore reasonable to infer that, from the crystallography data, the increased number of water molecules in *M. thermophila* laccase in the presence of DES result in an increase in hydrogen bonds, causing slight conformational changes that leads to increase in protein stability and changes in enzymatic activity.

The positive effects of DES on biocatalysis have been reported in several studies. For example, lysozyme in mixture of chlorine chloride: glycerol and water retained its structure with small differences in conformation compared to in pure buffer [66]. Molecular dynamics simulation has demonstrated that the hydrogen bond between glyceline (mixture of choline chloride: glycerol DES in a ratio of 1: 2) molecule and Trp-cage mini-protein results in a more rigid protein [72]. This study proves that the addition of LCDES (choline chloride: lactic acid) increases the catalytic activity of laccase with ABTS as the substrate. From the superimposed structure, the reaction of ABTS and laccase occurred on the surface, and this substantiates that the change in the catalytic activity of laccase in the presence of DES is due to the extra water molecules present.

### 3.5. Fluorescence spectroscopic analysis (Intrinsic fluorescence)

natural fluorophores. Generally, the exposed of tryptophan to the surrounding environment causes the emission spectra to red shift and a blue-shifted emission spectrum will appear when the tryptophan becomes embedded (from polar to a less polar environment) [73]. The emission maximum of tryptophan in water is at 350 nm and typically shifts to between 310 nm–324 nm in non-polar protein regions [74].

The intrinsic fluorescence study of *M. thermophilla* laccase with different concentrations of LCDES, LBDES, GCDES and GBDES excited at 295 nm is carried out to elucidate the effects of DES on the conformation of *M. thermophilla* laccase. The emission spectrum obtained solely demonstrated the behavior of tryptophan residue as the excitation is at 295 nm. The emission spectrums for LBDES, LCDES, GCDES and GBDES at different concentrations are shown in Fig. 8 with the maximum wavelength of different concentration of different DES summarized in Fig. 9. For *M. thermophilla* laccase (without DES), a single emission peak at 325 nm is observed, indicating the tryptophan residues are distributed between polar and non-polar environments. From Fig. 8, all the spectra red shifted upon the addition of DES, with LCDES shows the most prominent increase in maximum wavelength. In 5 % v/v and 10 % v/v of LCDES, the maximum fluorescence wavelength ($\lambda_{max}$) increases (red shifted) from ca. 325 nm to ca. 330 and ca. 335 nm respectively followed by the increase in intensity compared to the untreated laccase. At higher concentrations (20 % v/v and 30 % v/v), the emission intensity decreases considerably with a red shifted $\lambda_{max}$. The maximum fluorescence intensity in the presence of LBDES increases with increasing concentration of LBDES. For GCDES and GBDES, the $\lambda_{max}$ red-shifted slightly with increasing concentration, but the intensity fluctuates minimally in different concentrations of GCDES.

The red-shifted emission spectrum upon the addition of DES implies that DES induce conformational changes in *M. thermophilla* laccase, where the Trp residues are exposed to a different microenvironment. Generally, the emission spectrum reflects the nature of the microenvironment of the fluorophores [74]. Therefore, the changes in the emission maximum upon the addition of DES are the direct result of changes in the local environment of the Trp residues present in the protein. All DESs used in this study cause *M. thermophilla* laccase to have a more relaxed structure. Based on this result, the increase in water molecules in the presence of LCDES, as demonstrated in the crystal structure of the protein causes an increase in conformational flexibility, 'loosening' the protein structure. The results of intrinsic fluorescence validate previous hypothesis in kinetic studies where DES triggered conformational changes in *M. thermophilla* laccase. The spectroscopic and activity data indicates that *M. thermophila* laccase, a more relaxed structure triggers an increase in activity. However, the changes in protein compactness cannot be deduced based on the intensity (quantum yield) of the emission, especially on a multi-tryptophan protein. The emission intensity is affected by various factors, including the presence of amino acid side chains, peptide bonds, disulfides, and amides that act as fluorescence quenchers, resulting changes in fluorescence intensity [74,75]. As *M. thermophilla* laccase is a multi-tryptophan protein (15 Trp), it is difficult to distinguish the exact Trp residue that contributes to the changes in the spectroscopic signal as each Trp residue contributes unequally to the total emission.

### 3.6. Circular dichroism spectroscopy

Circular dichroism was used to determine the changes in the secondary structure of *M. thermophilla* laccase after being exposed to GCDESs at different concentrations. However, we were unable to analyze CD spectra for GBDES and lactic acid-based DES (both LCDES and LBDES) due to high dynode voltage below ~215 nm and high noise to signal ratio in the CD signal. Therefore, only the CD spectra for GCDES at different concentrations were recorded and analyzed, as the signal to

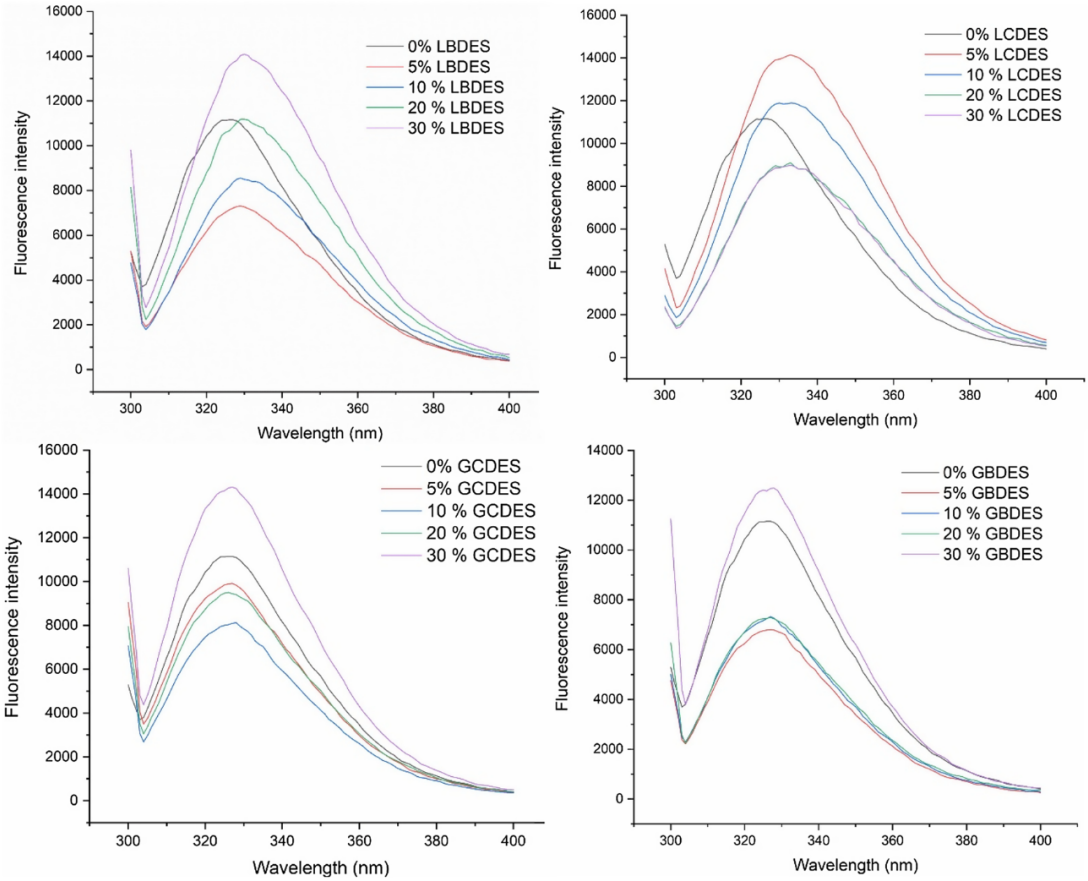


**Fig. 8.** Fluorescence emission spectra at different concentration of LBDES, LCDES, GCDES and GBDES.

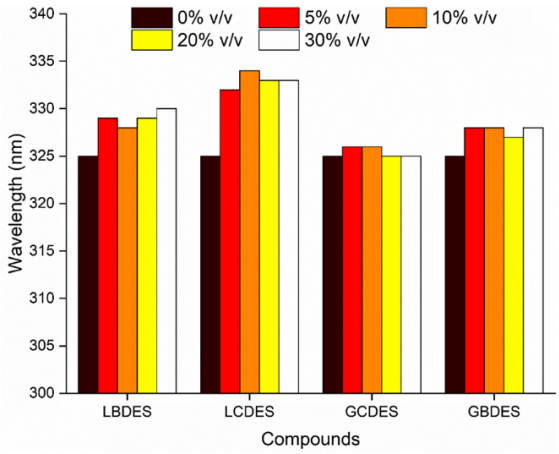


**Fig. 9.** Changes in wavelength for different concentrations of LBDES, LCDES, GCDES, GBDES.

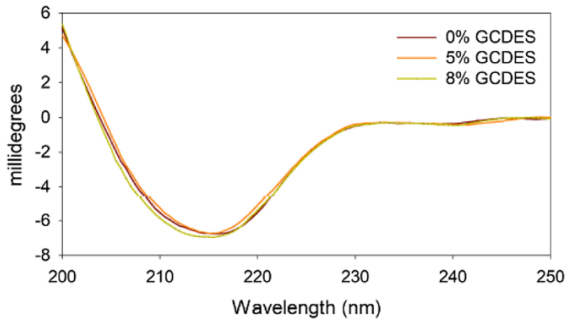


**Fig. 10.** *M. thermophila* laccase structure resulted in a slight increase in disorderness in presence of different concentrations of GCDES. Effect of spectra for laccase under different concentration of GCDES was measured in 50 mM sodium acetate buffer pH 5.0 at 25 °C. Shift of the minimum to lower wavelengths indicates slight increase in structural disorder.

216 nm (Fig. 10), which is close to the 218 nm minimum in CD spectra of β-sheet structure proteins [76]. These findings are in agreement with the three-dimensional structure of *M. thermophila* laccase obtained in the previous section. From the Figure, the minimum shifted to lower wavelengths (~215 nm) as the concentration of GCDES increased. CD spectra of random coil containing peptides has a strong negative signal slight increase in random coil content indicating loss of structure in certain specific region in the presence of GCDES. This is consistent with the decrease in activity observed previously.

## 4. Conclusion

The present study determined the effects of different DESs on laccase activity. GCDES and LCDES showed inhibitory effects on *M. thermophila*

concentration of GCDES revealed that GCDES acts as a S-parabolic-I-parabolic mixed non-competitive inhibitor (non-linear inhibitor) and there are multiple binding sites exist on *M. thermophila* laccase. Crystallographic structural analysis of *M. thermophila* laccase crystal soaked in LCDES showed that there is an increase in the number of bound water molecules in the structure, causing changes in the local environment of the amino acid, leading to structural changes of the protein. Both kinetic and structural study of *M. thermophila* laccase in the presence of DES demonstrated that DES induces conformational changes which can promote protein folding and affect enzyme activity and thermostability. Lactic acid based DESs possess high activation effects, owing to the self-hydrogen bonds formed in addition to the hydrogen bonds present in DES, which, in turns, causes the significant elevation in laccase activity. These results provide new understandings toward application of laccase with DES for biomass processing.

## CRediT authorship contribution statement

**Jou Chin Chan:** Data curation, Conceptualization, Visualization, Writing - original draft. **Bixia Zhang:** Data curation, Software, Methodology. **Michael Martinez:** Methodology. **Balaganesh Kuruba:** Methodology. **James Brozik:** Supervision. **ChulHee Kang:** Funding acquisition, Writing - review & editing, Supervision. **Xiao Zhang:** Conceptualization, Funding acquisition, Writing - review & editing, Supervision.

## Declaration of Competing Interest

The authors report no declarations of interest.

## Acknowledgements

The authors are grateful for the support from the Murdock Charitable Trust, NSF (CHE 1804699) and National Science Foundation [grant number 1454575] for funding part of this work. This research used resources of the Advanced Light Source (beamline 5.0.2), which is a DOE Office of Science User Facility under contract no. DE-AC02-05CH11231. Molecular graphics and analyses are performed with UCSF Chimera, developed by the Resource for Biocomputing, Visualization, and Informatics at the University of California, San Francisco, with support from NIH P41-GM103311. The authors would like to thank Novozymes North America for providing the laccase enzymes. The authors thank Dr. Alla Kostyukova for discussing the CD data.

## Appendix A. Supplementary data

Supplementary material related to this article can be found, in the online version, at doi:https://doi.org/10.1016/j.enzmictec.2021.109890.

## References

[1] A.S. Bommarius, B.R. Riebel-Bommarius, Biocatalysis: Fundamentals and Applications, John Wiley & Sons, 2004.
[2] P.F. Lindley, G. Card, I. Zaitseva, et al., An X-Ray structural study of human ceruloplasmin in relation to ferroxidase activity, Jbic J. Biol. Inorg. Chem. 2 (4) (1997) 454–463.
[3] A. Messerschmidt, R. Ladenstein, R. Huber, et al., Refined crystal structure of ascorbate oxidase at 1.9 Å resolution, J. Mol. Biol. 224 (1) (1992) 179–205.
[4] J.C. Chan, M. Paice, X. Zhang, Enzymatic oxidation of lignin: challenges and barriers toward practical applications, ChemCatChem 12 (2) (2019) 401–425.
[5] A. Leonowicz, N. Cho, J. Luterek, et al., Fungal laccase: properties and activity on lignin, J. Basic Microbiol. 41 (3–4) (2001) 185–227.
[6] P. Baldrian, Fungal laccases–Occurrence and properties, FEMS Microbiol. Rev. 30 (2) (2006) 215–242.
[9] F. Xu, Oxidation of phenols, Anilines, and Benzenethiols by fungal laccases: correlation between activity and redox potentials as well as halide inhibition, Biochemistry 35 (23) (1996) 7608–7614.
[10] F. Xu, W. Shin, S.H. Brown, et al., A study of a series of recombinant fungal laccases and bilirubin oxidase that exhibit significant differences in redox potential, substrate specificity, and stability, Biochim. Biophys. Acta Prot. Struct. Mol. Enzym. 1292 (2) (1996) 303–311.
[11] N. Karaki, A. Aljawish, C. Humeau, et al., Enzymatic modification of polysaccharides: mechanisms, properties, and potential applications: a review, Enzyme Microb. Technol. 90 (2016) 1–18.
[12] P. Giardina, V. Faraco, C. Pezzella, et al., Laccases: a never-ending story, Cell. Mol. Life Sci. 67 (3) (2010) 369–385.
[13] V. Gupta, N. Capalash, P. Sharma, Laccases and their role in bioremediation of industrial effluents, in: R. Chandra (Ed.), Advances in Biodegradation and Bioremediation of Industrial Waste, CRC Press, 2015, pp. 111–140.
[14] F. Xu, in: M.C. Flickinger, S.W. Drew (Eds.), Laccase, in Encyclopedia of Bioprocess Technology: Fermentation, Biocatalysis, and Bioseparation, Wiley, New York, 1999, pp. 1545–1554.
[15] P. Bajpai, Application of enzymes in the pulp and paper industry, Biotechnol. Prog. 15 (2) (1999) 147–157.
[16] S. Camarero, D. Ibarra, A.T. Martinez, et al., Paper pulp delignification using laccase and natural mediators, Enzyme Microb. Technol. 40 (5) (2007) 1264–1271.
[17] A. Hüttermann, C. Mai, A. Kharazipour, Modification of lignin for the production of new compounded materials, Appl. Microbiol. Biotechnol. 55 (4) (2001) 387–394.
[18] O. Morozova, G. Shumakovich, S. Shleev, et al., Laccase-mediator systems and their applications: a review, Appl. Biochem. Microbiol. 43 (5) (2007) 523–535.
[19] E. Abadulla, T. Tzanov, S. Costa, et al., Decolorization and detoxification of textile dyes with a laccase from trametes hirsuta, Appl. Environ. Microbiol. 66 (8) (2000) 3357–3362.
[20] D.T. D'Souza, R. Tiwari, A.K. Sah, et al., Enhanced production of laccase by a marine fungus during treatment of colored effluents and synthetic dyes, Enzyme Microb. Technol. 38 (3–4) (2006) 504–511.
[21] S. Yagüe, M.C. Terrón, T. González, et al., Biotreatment of Tannin-Rich Beer-Factory Wastewater with White-Rot Basidiomycete Coriolopsis Gallica Monitored by Pyrolysis/Gas Chromatography/Mass Spectrometry, Rapid Commun. Mass Spectrom. 14 (10) (2000) 905–910.
[22] V. Ducros, A.M. Brzozowski, K.S. Wilson, et al., Crystal structure of the Type-2 Cu depleted laccase from coprinus cinereus at 2.2 Å resolution, Nat. Struct. Mol. Biol. 5 (4) (1998) 310–316.
[23] V. Madhavi, S. Lele, Laccase: properties and applications, BioResources 4 (4) (2009) 1694–1717.
[24] R. Hatti-Kaul, V. Ibrahim, Lignin-Degrading Enzymes: An Overview. Bioprocessing Technologies in Biorefinery for Sustainable Production of Fuels, Chemicals, and Polymers (2012) 167–192.
[25] R.C. Kuhad, A. Singh, K.-E.L. Eriksson, Microorganisms and enzymes involved in the degradation of plant fiber cell walls. Biotechnology in the Pulp and Paper Industry, Springer, 1997, pp. 45–125.
[26] F. Xu, Laccase. Encyclopedia of Bioprocess Technology, 1999.
[27] T. Bertrand, C. Jolivalt, P. Briozzo, et al., Crystal structure of a four-copper laccase complexed with an arylamine: insights into substrate recognition and correlation with kinetics, Biochemistry 41 (23) (2002) 7325–7333.
[28] S.M. Jones, E.I. Solomon, Electron transfer and reaction mechanism of laccases, Cell. Mol. Life Sci. 72 (5) (2015) 869–883.
[29] D.W. Wong, Structure and action mechanism of ligninolytic enzymes, Appl. Biochem. Biotechnol. 157 (2) (2009) 174–209.
[30] S. Sarmad, Y. Xie, J.-P. Mikkola, et al., Screening of deep eutectic solvents (Dess) as green Co 2 sorbents: from solubility to viscosity, New J. Chem. 41 (1) (2017) 290–301.
[31] M. Francisco, A. van den Bruinhorst, M.C. Kroon, New natural and renewable low transition temperature mixtures (Lttms): screening as solvents for lignocellulosic biomass processing, Green Chem. 14 (8) (2012) 2153–2157.
[32] A.P. Abbott, D. Boothby, G. Capper, et al., Deep eutectic solvents formed between choline chloride and carboxylic acids: versatile alternatives to ionic liquids, J. Am. Chem. Soc. 126 (29) (2004) 9142–9147.
[33] J.T. Gorke, F. Srienc, R.J. Kazlauskas, Hydrolase-catalyzed biotransformations in deep eutectic solvents, Chem. Commun. (10) (2008) 1235–1237.
[34] S. Khodaverdian, B. Dabirmanesh, A. Heydari, et al., Activity, stability and structure of laccase in betaine based natural deep eutectic solvents, Int. J. Biol. Macromol. 107 (2018) 2574–2579.
[35] Z.L. Huang, B.P. Wu, Q. Wen, et al., Deep eutectic solvents can Be viable enzyme activators and stabilizers, J. Chem. Technol. Biotechnol. 89 (12) (2014) 1975–1981.
[36] M.L. Toledo, M.M. Pereira, M.G. Freire, et al., Laccase activation in deep eutectic solvents, ACS Sustain. Chem. Eng. 7 (13) (2019) 11806–11814.
[37] D. Lindberg, M. de la Fuente Revenga, M. Widersten, Deep eutectic solvents (Dess) are viable cosolvents for enzyme-catalyzed epoxide hydrolysis, J. Biotechnol. 147 (3–4) (2010) 169–171.
[38] V. Stepankova, P. Vanacek, J. Damborsky, et al., Comparison of catalysis by Haloalkane Dehalogenases in aqueous solutions of deep eutectic and organic solvents, Green Chem. 16 (5) (2014) 2754–2761.
[39] B.-P. Wu, Q. Wen, H. Xu, et al., Insights into the impact of deep eutectic solvents on horseradish peroxidase: activity, stability and structure, J. Mol. Catal., B Enzym.

[41] M.M. Bradford, A rapid and sensitive method for the quantitation of microgram quantities of protein utilizing the principle of protein-dye binding, Anal. Biochem. 72 (1–2) (1976) 248–254.
[42] U.K. Laemmli, Cleavage of structural proteins during the assembly of the head of bacteriophage T4, Nature 227 (5259) (1970) 680–685.
[43] L. Gou, J. Lee, J.-M. Yang, et al., The effect of alpha-ketoglutaric acid on tyrosinase activity and conformation: kinetics and molecular dynamics simulation study, Int. J. Biol. Macromol. 105 (2017) 1654–1662.
[44] I.H. Segel, Enzyme Kinetics: Behavior and Analysis of Rapid Equilibrium and Steady State Enzyme Systems, Wiley, 1975.
[45] V. Leskovac, Comprehensive Enzyme Kinetics, Springer Science & Business Media, 2003.
[46] Z. Otwinowski, W. Minor, Processing of X-Ray diffraction data collected in oscillation mode, Methods Enzymol. 276 (1997) 307–326.
[47] P. Emsley, B. Lohkamp, W.G. Scott, et al., Features and development of coot, Acta Crystallogr. Sect. D. Biol. Crystallogr. 66 (4) (2010) 486–501.
[48] S. Riva, Laccases: blue enzymes for green chemistry, Trends Biotechnol. 24 (5) (2006) 219–226.
[49] J. Rodakiewicz-Nowak, Phenols oxidizing enzymes in water-restricted media, Top. Catal. 11 (1–4) (2000) 419–434.
[50] S.H. Kim, S. Park, H. Yu, et al., Effect of deep eutectic solvent mixtures on lipase activity and stability, J. Mol. Catal., B Enzym. 128 (2016) 65–72.
[51] H. Monhemi, M.R. Housaindokht, A.A. Moosavi-Movahedi, et al., How a protein can remain stable in a solvent with high content of urea: insights from molecular dynamics simulation of Candida antarctica lipase B in Urea: choline chloride deep eutectic solvent, Phys. Chem. Chem. Phys. 16 (28) (2014) 14882–14893.
[52] A. Gutiérrez, R. Alcalde, M. Atilhan, et al., Insights on betaine + lactic acid deep eutectic solvent, Ind. Eng. Chem. Res. (2020).
[53] Z. Yang, Natural deep eutectic solvents and their applications in biotechnology, in: T. Itoh, Y.-M. Koo (Eds.), Application of Ionic Liquids in Biotechnology, Springer International Publishing, Cham, 2018, pp. 31–59.
[54] R. Wahlström, J. Hiltunen, M.Pd.S.N. Sirkka, et al., Comparison of three deep eutectic solvents and 1-Ethyl-3-Methylimidazolium acetate in the pretreatment of lignocellulose: effect on enzyme stability, lignocellulose digestibility and one-pot hydrolysis, RSC Adv. 6 (72) (2016) 68100–68110.
[55] R.C. Diehl, E.J. Guinn, M.W. Capp, et al., Quantifying additive interactions of the osmolyte proline with individual functional groups of proteins: comparisons with urea and Glycine betaine, interpretation of M-Values, Biochemistry 52 (35) (2013) 5997–6010.
[56] B. Adamczak, M. Kogut, J. Czub, Effect of osmolytes on the thermal stability of proteins: replica exchange simulations of trp-cage in urea and betaine solutions, Phys. Chem. Chem. Phys. 20 (16) (2018) 11174–11182.
[57] G. Walsh, Biochemistry and Biotechnology, John Willey & Sons, 2002.
[58] P. Xu, G.-W. Zheng, M.-H. Zong, et al., Recent progress on deep eutectic solvents in Biocatalysis, Bioresour. Bioprocess. 4 (1) (2017) 34.
[59] V. Vagenende, M.G. Yap, B.L. Trout, Mechanisms of protein stabilization and prevention of protein aggregation by glycerol, Biochemistry 48 (46) (2009) 11084–11096.
[60] M. Alkazaz, V. Desseaux, G. Marchis-Mouren, et al., The Mechanism of Porcine Pancreatic A-Amylase: Kinetic Evidence for Two Additional Carbohydrate-Binding Sites, Eur. J. Biochem. 241 (3) (1996) 787–796.
[61] N. Yadav, K. Bhakuni, M. Bisht, et al., Expanding the potential role of deep eutectic solvents toward facilitating the structural and thermal stability of A-Chymotrypsin, ACS Sustain. Chem. Eng. 8 (27) (2020) 10151–10160.
[62] U.N. Dwivedi, P. Singh, V.P. Pandey, et al., Structure–Function relationship among bacterial, fungal and plant laccases, J. Mol. Catal., B Enzym. 68 (2) (2011) 117–128.
[63] Y. Levy, J.N. Onuchic, Water mediation in protein folding and molecular recognition, Annu. Rev. Biophys. Biomol. Struct. 35 (2006) 389–415.
[64] B. Prasad, K. Suguna, Role of water molecules in the structure and function of aspartic proteinases, Acta Crystallogr. Sect. D. Biol. Crystallogr. 58 (2) (2002) 250–259.
[65] S. Bandyopadhyay, S. Chakraborty, B. Bagchi, Secondary structure sensitivity of hydrogen bond lifetime dynamics in the protein hydration layer, J. Am. Chem. Soc. 127 (47) (2005) 16660–16667.
[66] A. Sanchez-Fernandez, K. Edler, T. Arnold, et al., Protein conformation in pure and hydrated deep eutectic solvents, Phys. Chem. Chem. Phys. 19 (13) (2017) 8667–8670.
[67] L.D. Barron, L. Hecht, G. Wilson, The lubricant of life: a proposal that solvent water promotes extremely fast conformational fluctuations in mobile heteropolypeptide structure, Biochemistry 36 (43) (1997) 13143–13147.
[68] M. Tarek, D. Tobias, Role of protein-water hydrogen bond dynamics in the protein dynamical transition, Phys. Rev. Lett. 88 (13) (2002) 138101.
[69] R.V. Dunn, R.M. Daniel, The use of gas–Phase substrates to study enzyme catalysis at low hydration, Philos. Trans. R. Soc. Lond., B, Biol. Sci. 359 (1448) (2004) 1309–1320.
[70] J. Yarwood, Hydration Processes in Biological and Macromolecular Systems: A General Discussion […] Was Held at Sheffield Hallam University, Sheffield, Uk on 1st, 2nd and 3rd April, 1996, Royal Society of Chemistry, 1996.
[71] L. Degrève, G. Brancaleoni, C. Fuzo, et al., On the role of water in the protein activity, Braz. J. Phys. 34 (1) (2004) 102–115.
[72] S. Pal, R. Roy, S. Paul, Potential of natural deep eutectic solvent, Glyceline, in the thermal stability of the trp-cage mini-protein, J. Phys. Chem. B (2020).
[73] S. Deshayes, G. Divita, Fluorescence technologies for monitoring interactions between biological molecules in vitro, Prog. Mol. Biol. Transl. Sci. (2013) 109–143. Elsevier.
[74] J.R. Lakowicz, Principles of Fluorescence Spectroscopy, Springer Science & Business Media, 2013.
[75] C.A. Royer, Probing protein folding and conformational transitions with fluorescence, Chem. Rev. 106 (5) (2006) 1769–1784.
[76] S.M. Kelly, T.J. Jess, N.C. Price, How to study proteins by circular dichroism, Biochimica et Biophysica Acta (BBA)-Proteins and Proteomics 1751 (2) (2005) 119–139.
[77] D.H. Corrêa, C.H. Ramos, The use of circular dichroism spectroscopy to study protein folding, form and function, Afr. J. Biochem. Res. 3 (5) (2009) 164–173.